THE SHAPE OF THE RELATIVISTIC IRON Kα LINE FROM MCG−6-30-15 MEASURED WITH THE CHANDRA HETGS AND RXTE

JULIA C. LEE[1], KAZUSHI IWASAWA[2], JOHN C. HOUCK[1], ANDREW C. FABIAN[2], HERMAN L. MARSHALL[1],
CLAUDE R. CANIZARES[1]

ABSTRACT

We confirm the detection of the relativistically broadened iron Kα emission at 6.4 keV with simultaneous *Chandra* HETGS and *RXTE* PCA observations. Heavily binned HETGS data show a disk line profile with parameters very similar to those previously seen by *ASCA*. We observe a resolved narrow component with a velocity width $\sim 4700 \, \mathrm{km \, s^{-1}}$ (FWHM $\sim 11,000 \mathrm{km \, s^{-1}}$), that is most prominent, and narrower (FWHM $\sim 3600 \mathrm{km \, s^{-1}}$) when the continuum flux is high. It plausibly is just the blue wing of the broad line. We obtain a stringent limit on the equivalent width of an intrinsically narrow line in the source of 16 eV, indicating little or no contribution due to fluoresence from distant material such as the molecular torus. Variability studies of the narrow component show a constant iron line flux and variable width indicating the line may be originating from different kinematic regions of the disk.

Subject headings: galaxies: active; quasars: general; X-ray: general; individual MCG−6-30-15

1. INTRODUCTION

The discovery with *ASCA* of broad iron lines in active galactic nuclei (AGN; Tanaka et al. 1995, hereafter T95; Mushotzky et al. 1995; Nandra et al. 1997), which were predicted by Fabian et al. (1989), has opened the window for studying the innermost regions of the accretion flow and the strong gravity regime at about 10 gravitational radii (i.e. $10 r_g = 10 GM/c^2$) around a black hole (Fabian et al. 1995). At the present time this regime is only accessible to X-ray observations (optical and radio spectral line data from galactic nuclei probe matter at $\sim 10^5 r_g$), and the iron line is widely accepted to be a comparatively robust probe of the immediate environment closest to the supermassive black hole at the center of AGNs (see review by Fabian et al. 2000, and references therein).

The best studied source and first to show the most extreme broad ($\Delta v \sim 100,000 \mathrm{km \, s^{-1}}$, T95) iron Kα emission line is the luminous ($L_X \sim 10^{43} \mathrm{erg \, s^{-1}}$) Seyfert 1 galaxy MCG−6-30-15 at $z \sim 0.0078$. The long 4.5-d *ASCA* observation in 1994 which revealed the line to be broad also showed it to be skewed (T95; Iwasawa et al. 1996). The breadth and asymmetry of this line was subsequently confirmed by more long *ASCA* (Iwasawa et al. 1999, Shih, Iwasawa & Fabian 2002), *RXTE* (Lee et al. 1998, 1999) and *BeppoSAX* (Guainazzi et al. 1999) observations. The breadth of the line ($\sigma \sim 0.5$ keV; $W_{K\alpha} \sim 200 - 500$ eV) if interpreted to be due to Doppler and gravitational broadening is consistent with the presence of relativistically deep gravitational potentials at the center regions of AGN. Recently, Wilms et al. (2002) reported with *XMM-Newton* observations of MCG−6-30-15 during a "deep minimum" (e.g. Iwasawa et al. 1996) an extremely broad line with breadth extending between $\sim 3 - 7$ keV, confirming that the black hole is most probably rapidly spinning. See also Fabian et al. (2002) for results on a longer *XMM* look.

In this Letter, we present the *Chandra* HETGS and simultaneous *RXTE* observations of MCG−6-30-15 in order to as-

sess the narrow diskline component of the relativistically broadened Fe Kα emission and place limits on any intrinsically narrow core from distant (e.g. torus) material. Because the torus is very distant from the central black hole, we expect any line(s) arising from this region to have velocity widths $<< 2500 \, \mathrm{km \, s^{-1}}$ FWHM (the width of the Balmer lines in MCG−6-30-15; Reynolds et al. 1997), and therefore not likely to be resolved by the HETGS ($\Delta \lambda \sim 1800$ km s^{-1} at the iron Kα energies). We also apply the same procedure to the data as was applied to the *ASCA* data in T95, thereby clearly revealing the broad component in the *Chandra* data.

2. OBSERVATIONS

MCG−6-30-15 was observed with the *Chandra* High Energy Transmission Grating Spectrometer (HETGS; Canizares et al. 2002, in preparation) from 2000 April 5–6, and again from 2000 August 21–22 (Fig. 1). The total integration time was ~ 125 ks. The source varied by $\sim 50\%$ during each observation. Simultaneous *RXTE* observations were made between 2000 April 3–9, with 30 ks of usable data.

We reduce the spectral data from L1 (raw unfiltered event) files using IDL processing scripts which are similar to the standard CIAO processing. A more complete description is in Marshall, Canizares, & Schulz (2002). We restrict the event list to the nominal (0,2,3,4,6) grade set, and remove event streaks in the S4 chip (these are not related to the readout streak). Event energies are corrected for detector node-to-node gain variations. The zeroth order position is determined and the ±1 order events are extracted for source and background regions. Bad columns are eliminated, as well as data which are affected by detector gaps. The extracted MEG (HEG) events have bins 0.01Å (0.005Å), or an ACIS pixel. The instrument effective area is based on pre-flight calibration data. We have assessed the zeroth order pileup and find that the pileup fraction (defined to be the fraction of all frames that have events > 2 photons during that frame) is 86%. (The average count rates are

---

[1]MIT, Department of Physics and Center for Space Research, 77 Massachusetts Ave., NE80, Cambridge, MA 02139.

[2]Institute of Astronomy, University of Cambridge, Madingley Rd., Cambridge CB3 0HA U.K.

$\sim 1 \, \mathrm{cts \, s^{-1}}$ from 0th order, and $1 \, \mathrm{cts \, s^{-1}}$ from the total of all dispersed events.) Accordingly, only $0.04 \, \mathrm{cts \, s^{-1}}$ are expected in single photon events making useful spectroscopic information difficult to extract from zeroth order. We use the software package ISIS (Houck & DeNicola 2000) for the *Chandra* data analysis

We extract PCA (Proportional Counter Array) light curves and spectra from only the top Xenon layer using the FTOOLS 5.1 software. Data from layer 1 of PCUs 0, 2, and 4 are combined to improve signal-to-noise at the expense of slightly blurring the spectral resolution. Good time intervals were selected to exclude any earth or South Atlantic Anomaly (SAA) passage occulations, and to ensure stable pointing. We also filter out electron contamination events. L7-240 background data are generated using PCABACKEST V4.0C. The PCA response matrix for the *RXTE* data set was created using PCARSP V7.11. Background models and response matrices are representative of the most up-to-date PCA calibrations.
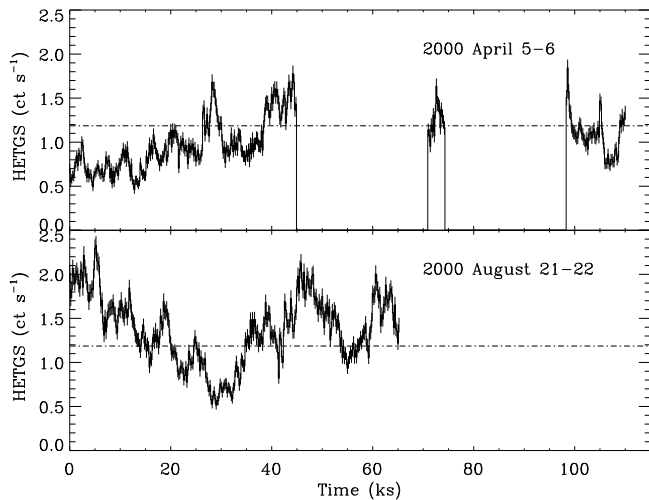

FIG. 1.— MCG−6-30-15 light curve (excluding 0th order) binned at 200 seconds. The dashed lines at $\sim 1.2 \, \mathrm{cts \, s^{-1}}$ denote the mean light curve count rate averaged over both observations. The 'high' and 'low' states discussed in §2.3 are defined respectively to be above and below this value.

2.1. *Spectral Results*

The *RXTE* PCA is better suited for constraining the continuum shape as a consequence of its wide band coverage. From these data, we obtain the best-fit photon index $\Gamma = 1.93 \pm 0.02$. These fits were performed in XSPEC with a simple Galactic ($4.06 \times 10^{20} \, \mathrm{cm^{-2}}$) absorbed power-law using the 3.3–4.6 keV and 8.0–10 keV spectral data ($\chi^2/dof = 5.96/6$). The 4.6–8 keV energy range were excluded in order that we may obtain the best description of Γ with minimal bias from the red wing of the broad iron line which can extend redwards to well below 5 keV (e.g. Fig. 3, Tanaka et al. 1995, Iwasawa et al. 1996), or even farther (e.g. Wilms et al. 2002, Fabian et al. 2002).

We next determined the power-law normalization which best describes the *Chandra* HETGS spectrum by fitting the MEG and HEG (respectively, medium and high energy grating) 3–4 keV data, with a power-law (Γ fixed at the best-fit *RXTE* value) modified by $2 \times 10^{21} \, \mathrm{cm^{-2}}$ absorption (to accomodate the warm absorber which has $\lesssim 3\%$ effect at 3 keV, and no effect at $\gtrsim 4$ keV). This limited energy range was chosen in order to avoid contamination from the absorption features attributed to the warm absorber below 3 keV (e.g. Lee et al. 2001, Sako et al. 2002) and the broad Fe Kα emission above 4 keV. The

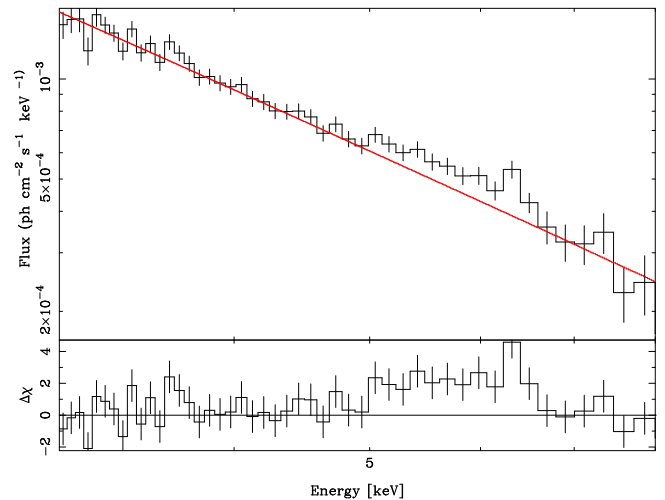continuum is defined as the extrapolation of this fit to include energies to 8 keV.

FIG. 2.— The power-law continuum described in §2.1 over-plotted on the HEG spectrum of MCG−6-30-15. The data have been heavily binned (0.055 Å) in order to emphasize the excess emission between $\sim 5 - 6.5$ keV that is attributed to the relativistically broadened Fe Kα emission.
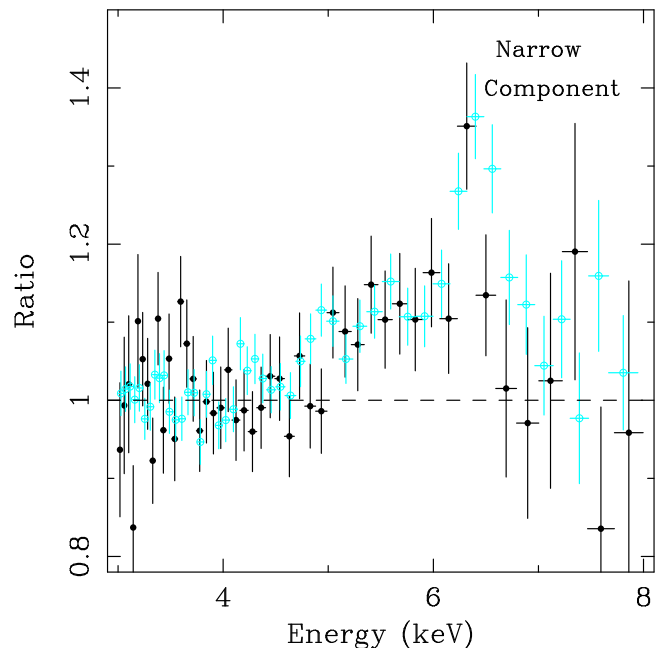

FIG. 3.— The iron Kα emission profile from the long (4.5 day) *ASCA* observation (Tanaka et al., 1995) in blue open circles, superposed on the heavily binned *Chandra* HEG spectrum (black filled circles) show that the line is broad and skewed, extending far into the red.

2.2. *The relativistic diskline*

Fig. 2 illustrates the power-law continuum described previously over-plotted on the binned (0.055 Å) HEG spectrum − notice the clear excess between 5 and 6.6 keV. The corresponding ratio plot of data−to−model in Fig. 3 further shows that the heavily binned *Chandra* data reveals a line profile very similar to that first discovered by T95. We note, however, that since a simple power-law is used to derive the line profile seen in this figure, it is possible that some fraction of the broad ex-

cess at ~ 5 keV can have contributions from the reflection spectrum known to exist in this source (e.g. Lee et al. 1998, 1999).

To further investigate the degree to which the relativistic disk line can account for the line profile of Fig. 3, we fit the *Chandra* data with a power-law plus diskline model modified by absorption. The power-law component is that described previously and the diskline parameters are fixed at the T95 values : accretion disk at inclination $i = 30°$, respectively inner ($R_{in} = 3.4R_S$) and outer ($R_{out} = 10R_S$) radii , line energy = 6.35 keV (6.4 keV in the galaxy frame), and radial emissivity $\alpha = 3$ assuming a power-law-type emissivity function $\propto R^{-\alpha}$ of the line. This model gives $\chi^2/d.o.f = 42/47$, and Fe Kα flux $(1.37 \pm 0.29) \times 10^{-4}\,\mathrm{ph\,cm^{-2}\,s^{-1}}$, with equivalent width $W_{K\alpha} \sim 295 \pm 118$ eV. This is in good agreement with the broad iron line measured using the *RXTE* data which has $W_{K\alpha} = 398 \pm 58$ eV, comparable to previous *RXTE* (e.g. Lee et al. 1998, 1999) and *ASCA* measurements of this source (e.g. Iwasawa et al. 1996, 1999). The apparent 'sharp drop' at 6.7 keV (Fig. 3) appears resolved ($\Delta E > 70$ eV from peak to drop). A simple Galactic absorbed power-law (as discussed previously) plus Gaussian fit to the *RXTE* data gives $E_{K\alpha(obs)} = 6.21 \pm 0.08$ keV, Gaussian width $\sigma = 0.66 \pm 0.11$ (FWMH $\sim 73,000$ km s^{-1}), and iron line flux $I_{K\alpha} = (2.13 \pm 0.31) \times 10^{-4}\,\mathrm{ph\,cm^{-2}\,s^{-1}}$.
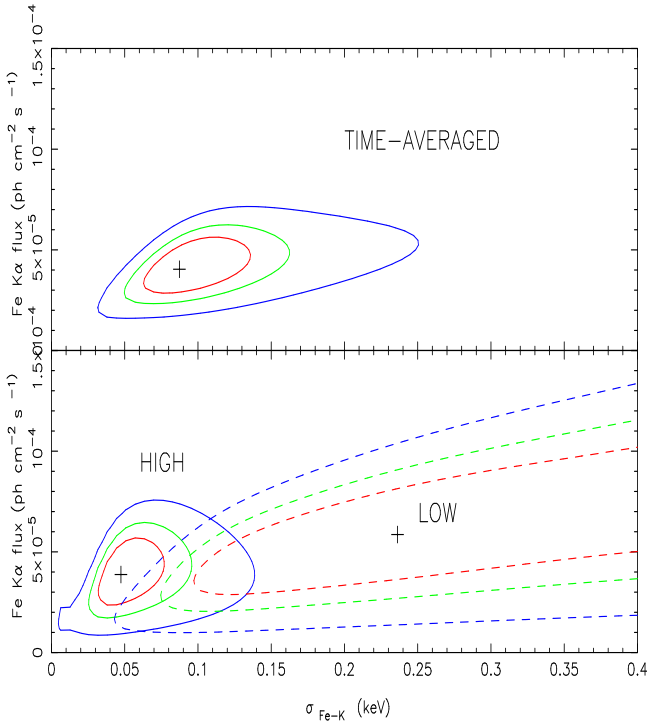

FIG. 4.— Respectively from inner to outer contour, 68, 90, 99 per cent confidence limits on the iron Kα narrow core. The bottom panel shows the comparison of high (solid) versus low (dashed) state.

2.3. *The Fe Kα narrow component*

We next address the formal detectability of the iron line narrow component and resolution of its width. We note that the count rate of the full 125 ks observation at the iron line energies is $\sim 20 - 30$ cts bin^{-1} (where bin = 0.005Å, or an ACIS pixel) and therefore sufficient for statistically meaningful errors derived from spectral fitting. Table 1 shows the narrow component parameters when fitting a Gaussian to the residuals of the best fit power law described in §2.1 (see also Fig. 5). The

68, 90, and 99% confidence contours (3 free parameters and 515 degrees of freedom) of Fig. 4 show that the narrow component is resolved at 99% confidence with a full width at half maximum (FWHM) $\sim 11,000$ km s^{-1} based on the full observation, and ~ 3600 km s^{-1} from the 'high' continuum flux period (see below). (The statistical significance of the excess counts in the narrow component over a power law plus 10% to account for the broad component is $> 99.9\%$.) The line strengths shown in Table 1 are consistent with those found for the narrow core by Iwasawa (1996, 1999). Wilms et al. (2002) report an "unresolved" (at the *XMM* EPIC resolution which is $\lesssim 4\times$ the *Chandra* HEG at the iron energies) narrow iron line with $W_{K\alpha} = 38$ eV. Fabian et al. (2002) attribute this to the blue wing of the disk line.

If there is a constant narrow core due to fluorescence from material far from the black hole, such as a molecular torus, then it should not vary during our observation and be strongest during the period of low continuum flux. To test for the presence of an intrinsically narrow core, we assess the variability nature of the narrow component, by separating the data into a 'high' (67 ks; 0.4-10 keV unabsorbed flux $f_{high} = 5 \times 10^{-11}\,\mathrm{erg\,cm^{-2}\,s^{-1}}$) and 'low' (58 ks; $f_{low} = 3 \times 10^{-11}\,\mathrm{erg\,cm^{-2}\,s^{-1}}$) flux states arbitrarily defined as above and below the mean count rate (Fig. 1) of the time averaged 125 ks ($f_{(0.4–10\,keV)} = 4 \times 10^{-11}\,\mathrm{erg\,cm^{-2}\,s^{-1}}$) observation. To ensure that there are sufficient counts, these data were binned to 0.01 Å to create the contour plots corresponding to the 'low' and 'high' state shown in Fig. 4. It can be seen that the region of overlap between these states exists only between the 90% confidence contours. This would indicate that the joint probability is $\sim 1\%$ that the iron line narrow component is a narrow core from distant material. This is depicted in Fig. 5 which shows that a comparison of the high versus low flux data against the best fit power-law model reveals that the iron line narrow component is effectively absent from the low flux state; σ could not be well constrained during this state because a very broad line (FMHM $\gtrsim 20,000$ km s^{-1}) is required by the fit. We note the features blue-ward of 6.5 keV (e.g. at ~ 6.82 keV) seen during the high and low states are only marginally ($\lesssim 2\sigma$) significant.

TABLE 1
PARAMETERS OF THE Fe Kα RESOLVED NARROW COMPONENT

Parameter	[a] ALL	[b] HIGH
Exposure	125 ks	67 ks
Restframe energy (keV)	$6.40^{+0.04}_{-0.05}$	$6.39^{+0.03}_{-0.02}$
Line flux (10^{-5} ph cm^{-2} s^{-1})	$4.2^{-1.6}_{+1.4}$	$3.0^{+1.6}_{-1.5}$
Gaussian width σ (keV)	$0.10^{+0.04}_{-0.04}$	$0.03^{+0.03}_{-0.02}$
Velocity width (km s^{-1})	5000^{+2000}_{-2000}	1500^{+1400}_{-700}
FWHM (km s^{-1})	11000^{+4600}_{-4700}	3600^{+3300}_{-2000}
Equivalent width (eV)	110^{+38}_{-40}	62^{+33}_{-30}
χ^2 / dof	562/ 515	586 / 515

Fits are assessed using the HEG data and errors are quoted at 90% confidence. [a] Data bins are 0.005Å. Note that we were unable to constrain the velocity width of the narrow component during the low state.

Using the 125 ks observation, we can set limits on the unresolved core by fixing the line energy at 6.4 keV and σ to the resolution of the HEG ($\sim 1800\,\mathrm{km\,s^{-1}}$ FWHM) at that energy, and assessing the 90% confidence for the line flux. The upper limit on an intrinsically narrow core is estimated to be $F_{\mathrm{K}\alpha} \sim 6 \times 10^{-6}\,\mathrm{ph\,cm^{-2}\,s^{-1}}$, fractionally $< 15\%$ of the line strength for the narrow component shown in Table 1.
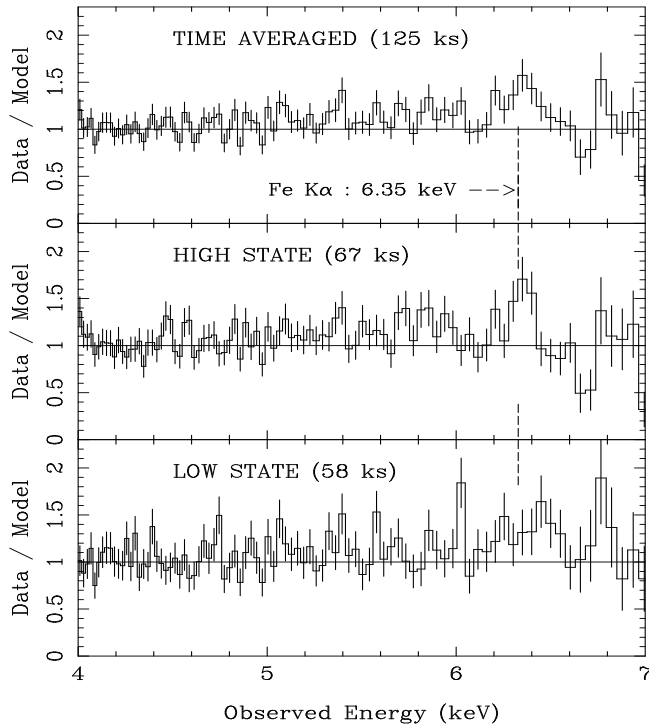

FIG. 5.— Ratio of data : power-law model shows that the Fe Kα narrow core is more prominent during the high state. Note that 6.35 keV is the observed energy of the 6.4 keV Fe Kα fluorescent emission in the rest frame of MCG−6-30-15. Data bins are 0.015Å.

3. DISCUSSION

A clear measurement of the iron line narrow component with *Chandra* has implications for resolving differences in the interpretation of the breadth and origin of the iron line in MCG−6-30-15. This pertains specifically to whether part of the iron line originates from a torus outside the broad line region (Ghisellini, Haardt & Matt 1994; Yaqoob et al. 2001, Reeves et al. 2001), as opposed to the blue horn of the relativistic diskline.

The possibility is small that a significant fraction of the broad line in MCG−6-30-15 is due to some distant material (e.g. a torus) based on the *Chandra* HEG data. It is more likely that the resolved narrow component is consistent with being the blue peak of a diskline (or possibly emission from the outer radii of the concave disk proposed by Blackman 1999). In particular, the *Chandra* HETGS data resolves the narrow component of

the $F_{\mathrm{K}\alpha}$ emission at 6.4 keV (6.35 keV observed) with a velocity width $\sim 4700\,\mathrm{km\,s^{-1}}$ (FWHM $\sim 11,000\,\mathrm{km\,s^{-1}}$). It has an $W_{\mathrm{K}\alpha} \sim 110$ eV, and is most pronounced when the continuum flux is high (FWHM $\sim 4000\,\mathrm{km\,s^{-1}}$).

- The resolved narrow component of the $F_{\mathrm{K}\alpha}$ emission seen in the HEG data of MCG−6-30-15 is significantly broader than expected from a torus outside the BLR (e.g. as seen in NGC 5548 with the HETGS – Yaqoob et al. 2001, or Markarian 205 with *XMM* EPIC – Reeves et al. 2001).

- Since the torus is thought to be $\gtrsim 1$ pc from the central source, reflection from this region should remain constant at average intensity levels. Therefore, we expect that such a component would be especially pronounced when the continuum flux is low. Yet, the narrow component is virtually absent from the low flux state in our data. This is consistent with the findings from *ASCA* data (Iwasawa et al. 1996, 1999).

- The 90% confidence limit on an intrinsically narrow core is $F_{\mathrm{K}\alpha} \sim 6 \times 10^{-6}\,\mathrm{ph\,cm^{-2}\,s^{-1}}$, fractionally $< 15\%$ of the line strength of the narrow component, or ~ 16 eV. This is significantly less than the ~ 60 eV found for the intrinsically narrow line thought to be from distant material found in the Seyfert 1.9 MCG−5-23-16 (Weaver et al. 1997).

- The difference in the iron line between the periods of low versus high continuum flux is seen in the width rather than the flux in the line. This implies that the line cannot come from very distant material but that it comes from kinematically different (or kinematically variable) material in the low and high states.

In summary, the *Chandra* HETGS data of MCG−6-30-15 confirm the presence of a broad line, resembling in shape and strength the line seen first with *ASCA* (T95). The narrow component at ~ 6.4 keV is not narrow enough to be from distant matter and is plausibly the blue wing of a relativistic line. Any intrinsically narrow core has an equivalent width of less than 16 eV, a small fraction of the total resolved narrow component (see Table 1). This is less than 25% of that expected if the X-ray source illuminates a distant molecular torus as commonly expected from Seyfert galaxy unification models (see e.g. Ghisellini et al. 1994 and references therein).

REFERENCES

Blackman, E. G. 1999, MNRAS, 306, L25
Fabian, A. C., Iwasawa, K., Reynolds, C. S., & Young, A. J. 2000, PASP, 112, 1145
Fabian, A. C., Nandra, K., Reynolds, C. S., Brandt, W. N., Otani, C., Tanaka, Y., Inoue, H., & Iwasawa, K. 1995, MNRAS, 277, L11
Fabian, A. C., Vaughan, S., Nandra, K., Iwasawa K., Ballantyne, D.R., Lee, J.C., De Rosa, A., Turner, A., Young, A.J., 2002, MNRAS, submitted
Ghisellini, G., Haardt, F., & Matt, G. 1994, MNRAS, 267, 743

Guainazzi, M. et al. 1999, A&A, 341, L27
Houck, J.C., and DeNicola, L.A., 2000, ASP Conf. Ser., Vol 216, 591
Iwasawa, K. et al. 1996, MNRAS, 282, 1038
Iwasawa, K., Fabian, A. C., Young, A. J., Inoue, H., & Matsumoto, C. 1999, MNRAS, 306, L19
Lee, J. C., Fabian, A. C., Brandt, W. N., Reynolds, C. S., & Iwasawa, K. 1999, MNRAS, 310, 973

Lee, J. C., Fabian, A. C., Reynolds, C. S., Brandt, W. N., & Iwasawa, K. 2000, MNRAS, 318, 857

Lee, J. C., Fabian, A. C., Reynolds, C. S., Iwasawa, K., & Brandt, W. N. 1998, MNRAS, 300, 583

Lee, J. C., Ogle, P. M., Canizares, C. R., Marshall, H. L., Schulz, N. S., Morales, R., Fabian, A. C., & Iwasawa, K. 2001, ApJ, 554, L13.

Marshall, H. L., Canizares, C. R., & Schulz, N. S. 2002, ApJ, 564, 941

Mushotzky, R. F., Fabian, A. C., Iwasawa, K., Kunieda, H., Matsuoka, M., Nandra, K., & Tanaka, Y. 1995, MNRAS, 272, L9

Nandra, K., George, I. M., Mushotzky, R. F., Turner, T. J., & Yaqoob, T. 1997, ApJ, 477, 602

Reeves, J. N., Turner, M. J. L., Pounds, K. A., O'Brien, P. T., Boller, T., Ferrando, P., Kendziorra, E., & Vercellone, S. 2001, A&A, 365, L134.

Reynolds, C. S., Ward, M. J., Fabian, A. C., & Celotti, A. 1997, MNRAS, 291, 403.

Sako, M., et al., 2002, ApJ, submitted (astro-ph/0112436)

Shih, D. C., Iwasawa, K., Fabian, A. C., 2002, MNRAS, in press

Tanaka, Y. et al. 1995, Nature, 375, 659

Weaver, K. A., Yaqoob, T., Mushotzky, R. F., Nousek, J., Hayashi, I., & Koyama, K. 1997, ApJ, 474, 675

Wilms, J., Reynolds, C. S., Begelman, M. C., Reeves, J., Molendi, S., Stuabert, R., Kendziorra, E., 2002, MNRAS, in press

Yaqoob, T., George, I. M., Nandra, K., Turner, T. J., Serlemitsos, P. J., & Mushotzky, R. F. 2001, ApJ, 546, 759